Journal of Ceramic Processing Research. Vol. 23, No. 2, pp. 109~112 (2022)
(Received 24 February 2021, Received in revised form 21 May 2021, Accepted 17 July 2021)
https://doi.org/10.36410/jcpr.2022.23.2.109

J O U R N A L O F
Ceramic Processing Research

The influence of Ca doping on the capacity fading of $LiNi_{0.8}Co_{0.1}Mn_{0.1}O_2$ cathode material

Chea-Yun Kang and Seung-Hwan Lee*
Department of Materials Science and Engineering, Kangwon National University, Chuncheon 24341, Republic of Korea

Ni-rich layered material can be regarded as an one of the promising cathode for high-energy lithium ion batteries. In this paper, Ca-doped Ni-rich $LiNi_{0.8}Co_{0.1}Mn_{0.1}O_2$ cathode material is prepared to investigate the effect of Ca doping on the structural properties and electrochemical performances. In structural properties, there is no obvious difference between the two samples in terms of crystallinity or morphology. In electrochemical performances, the initial capacity and electrochemical behavior are almost identical, while the degree of capacity deterioration in long-term cycle performance is obviously different. This is because Ca doping can increase the bond dissociation energy and pathways for electrons and lithium ions.

Keywords: Ni-rich layered material, High-energy lithium ion batteries, Ca-doped Ni-rich $LiNi_{0.8}Co_{0.1}Mn_{0.1}O_2$, Binding energy, Pathways for electrons and lithium ions.

Introduction

Recently, rechargeable lithium-ion batteries have been widely used in various applications such as electric vehicles (EVs), hybrid electric vehicles (HEVs) and uninterruptible power supply (UPS) owing to its high power and energy densities [1]. The Ni-rich ternary cathode material of layered structured $LiNi_{0.8}Co_{0.1}Mn_{0.1}O_2$ (NCM811) is one of the most attractive cathodes to replace $LiCoO_2$ due to its good cost-effectiveness, excellent high capacity and superior thermal stability [2]. Nevertheless, the high Ni-containing cathodes still need to improve structural deformation and rapid capacity decay, resulting from reaction with the electrolyte [3].

In order to enhance the electrochemical performance of $LiNi_{0.8}Co_{0.1}Mn_{0.1}O_2$ cathode, various effective methods have been developed. Surface coating, like Cd [4], SiO_2 [5], ZrO_2 [6], $AlPO_4$ [7], is a feasible way to achieve the excellent rate capability and good cyclability of $LiNi_{0.8}Co_{0.1}Mn_{0.1}O_2$ cathode. The surface coating layer can reduce side reactions which occurs at the electrolyte/electrode interface by preventing the cathode material from direct contact with the electrode [8]. Another effective approach to overcome inherent issues is to substitute Ni ions with cations, such as Mg [9], Al [8], Zr [10], Ca [11] and so on. Besides, these dopants are beneficial for increasing the lithium layer spacing, allowing fast lithium-ion diffusion into the electrode and improving structural stability during cycling [12]. It was reported that Ca doping can effectively reduce the cation disordering and enhance the electrochemical performances [11].

Therefore, in this work, we synthesized using a co-precipitation method to confirm the effect of Ca doping on the bulk and electrochemical performance for Ni-rich $LiNi_{0.8}Co_{0.1}Mn_{0.1}O_2$ cathode. The results exhibited that Mg doping can effectively enhance the electrochemical performance of $LiNi_{0.8}Co_{0.1}Mn_{0.1}O_2$ cathode.

Experimental

Experimental spherical $LiNi_{0.8}Co_{0.1}Mn_{0.1}O_2$ powder was fabricated through the general co-precipitation method. The appropriate amounts of nickel sulfate ($NiSO_4 \cdot 6H_2O$), cobalt sulfate ($CoSO_4 \cdot 7H_2O$) and manganese sulfate ($MnSO_4 \cdot 5H_2O$) were employed as the starting materials. At the same time, NaOH and NH_4OH were used as precipitating agents. The resulting $Ni_{0.8}Co_{0.1}Mn_{0.1}(OH)_2$ precursor was mixed with $LiOH \cdot H_2O$ in a LiOH/metal hydroxide mixture (1.05 ratio). Later, the obtained mixture was preheated at 550 ºC and for 6 h and sintered at 800 ºC 12 h, respectively with a heating rate of 4 ºC in a tube furnace under the O_2 atmosphere. For the synthesis of Ca-doped $LiNi_{0.8}Co_{0.1}Mn_{0.1}O_2$ cathode, LiOH (1:1.05) and $CaHPO_4$ were mixed in a molar ratio of 0.5 wt% and then sintered using above mentioned heating process.

For slurry casting process, the cathode prepared by mixing cathode powder, conductive carbon black and polyvinylidene fluoride (PVDF) binder at a weight ratio of 96:2:2, and then adding N-methyl-pyrrolidinone (NMP) solvent to obtain homogeneously slurry. After that, the prepared slurry was coated on an Al foil and then heated at 120 ºC for 10 h to remove NMP solvent

*Corresponding author:
Tel : +82-42-280-2414
E-mail: shlee@kangwon.ac.kr

in a vacuum oven. The coin cells were assembled in an Ar-filled glove box using lithium foil as an anode. 1M solution of LiPF6 in an organic solvent (ethylene carbonate/dimethyl carbonate/ethyl methyl carbonate, with a volumetric ratio of 1 : 1 : 1) was employed as electrolyte.

Structure properties of the samples were confirmed via X-ray diffraction. The microstructures and elements of the resulting samples were confirmed by using field emission electron microscopy (FE-SEM, Hitachi S-4800) with energy dispersive X-ray spectrometry (EDS). The electrochemical performances were performed via electrochemical equipment (TOSCAT-3100, Toyo system).

Results and Discussion

Fig. 1 shows the XRD patterns of the pristine and Ca-doped $LiNi_{0.8}Co_{0.1}Mn_{0.1}O_2$ materials. It can be observed that both samples have same peak positions of typical Ni-rich $LiNi_{0.8}Co_{0.1}Mn_{0.1}O_2$. It means they have layered hexagonal structure with α-$NaFeO_2$ structure with the space group R-3m (JCPDS No. 41-0324)

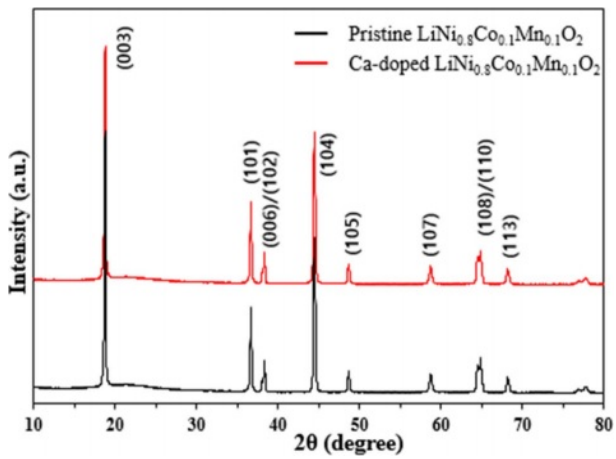

Fig. 1. XRD patterns of pristine and Ca-doped $LiNi_{0.8}Co_{0.1}Mn_{0.1}O_2$.

[13, 14]. It can be explained by very small amount of C concentration. Both samples deliver similar I(003)/I(104) ratio and ratios of Ca-doped $LiNi_{0.8}Co_{0.1}Mn_{0.1}O_2$ and pristine $LiNi_{0.8}Co_{0.1}Mn_{0.1}O_2$ are 1.41 and 1.37, respectively. Both samples have good layered structure because the I(003)/I(104) ratio is higher than 1.2. Moreover, the obvious peak splitting of (006)/(102) and (108)/(110) for both samples also demonstrates well-ordered layered structure. From these, we can infer that Ca-doped $LiNi_{0.8}Co_{0.1}Mn_{0.1}O_2$ has relatively lower Li^+/Ni^{2+} cation disordering, since it is well known that cation mixing is closely related to the deformation of the layered structure of Ni-rich $LiNi_{0.8}Co_{0.1}Mn_{0.1}O_2$. The improved cation mixing is explained by replacing Ni site in Ca-doped $LiNi_{0.8}Co_{0.1}Mn_{0.1}O_2$ with Ca, leading to fast Li ion kinetics [15, 16]. The enlarged (003) diffraction peak indicates that Ca is successfully doped into the crystal lattice of pristine $LiNi_{0.8}Co_{0.1}Mn_{0.1}O_2$. The (003) peak of Ca-doped $LiNi_{0.8}Co_{0.1}Mn_{0.1}O_2$ is shifting toward lower Bragg angle since ionic radius of Ca (0.99 Å) is larger than that of Ni^{2+} (0.56Å) [17].

Fig. 2 delivers the microstructures of the pristine and Ca-doped $LiNi_{0.8}Co_{0.1}Mn_{0.1}O_2$ materials. Both samples exhibit typical spherical morphology with average size in the rage from 8-10 μm. Such secondary particle is composed of a lot of nanoparticles as primary particles. The grain sizes ranged from 100-300 nm. There is no big difference between both samples. We can conclude that Ca dopant does not change the microstructures such as shape and size of pristine $LiNi_{0.8}Co_{0.1}Mn_{0.1}O_2$ materials. It is reported that such porous structure of both samples allows for smooth and fast Li ion transfer via sufficient soaking of liquid electrolyte [18]. These structural properties can affect the electrochemical performances.

Fig. 3 shows the EDS mapping of Ca-doped $LiNi_{0.8}Co_{0.1}Mn_{0.1}O_2$ to support existence of Ca doping into the NCM. We can observe the uniform dispersion of Ni, Co, Mn and Ca elements throughout the particles.

For electrochemical tests, pristine and Ca-doped

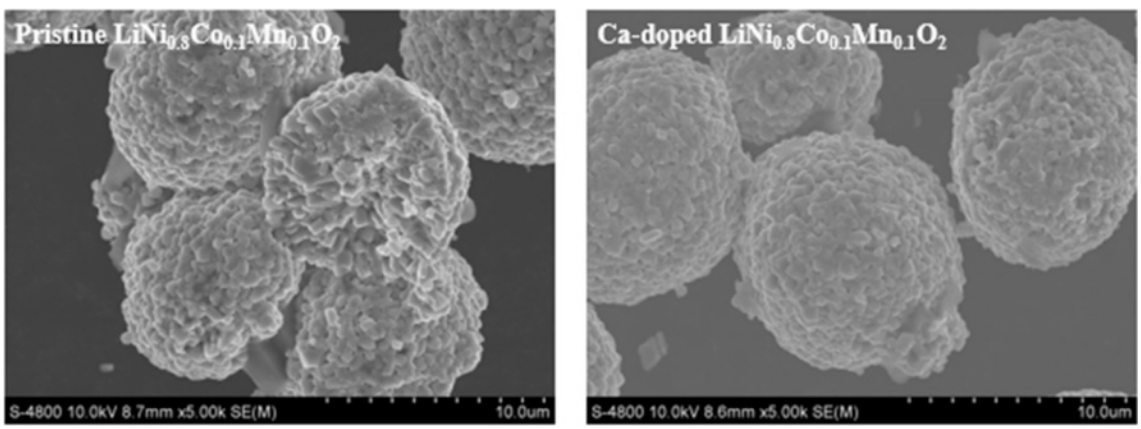

Fig. 2. Microstructures of pristine and Ca-doped $LiNi_{0.8}Co_{0.1}Mn_{0.1}O_2$.

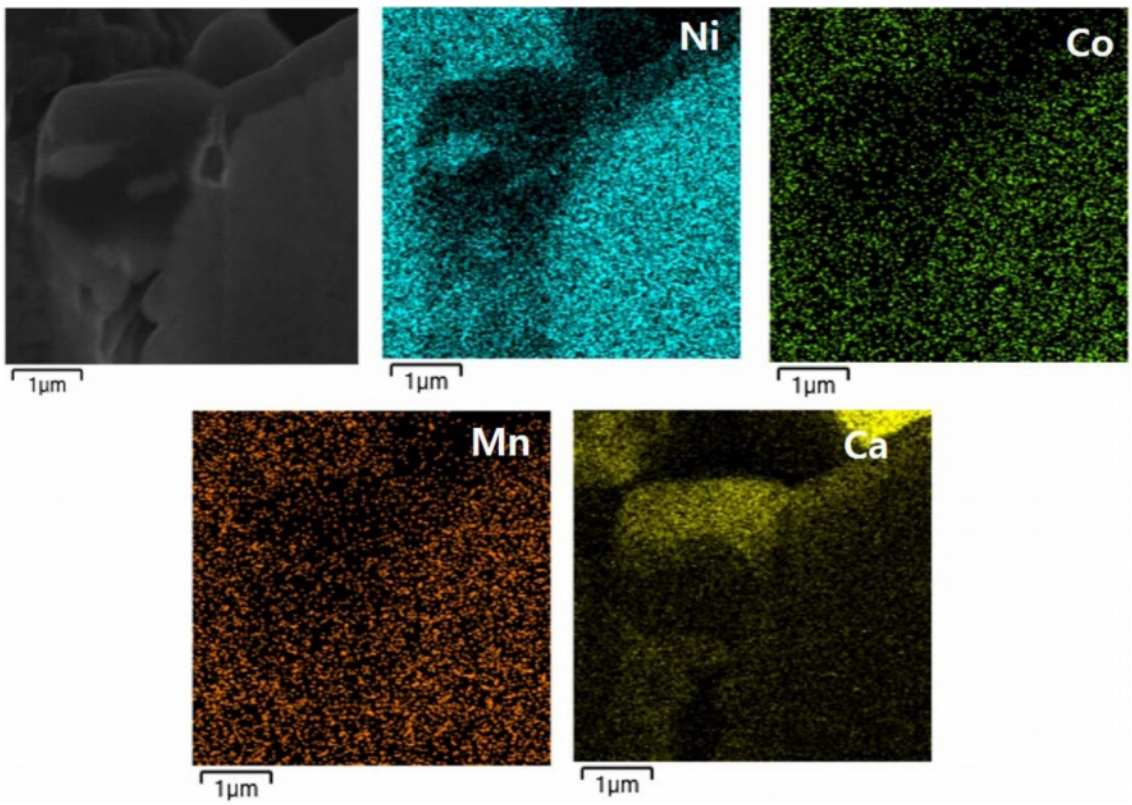

Fig. 3. EDS mapping images of Ca-doped $LiNi_{0.8}Co_{0.1}Mn_{0.1}O_2$

$LiNi_{0.8}Co_{0.1}Mn_{0.1}O_2$ are fabricated in thick electrode laminates with high areal loading of active materials (approximately 14.5 mg/cm^2), to confirm the applicability to commercial lithium ion batteries [19]. The long-term cycle stabilities of pristine and Ca-doped $LiNi_{0.8}Co_{0.1}Mn_{0.1}O_2$ are shown in Fig. 4. The initial discharge of Ca-doped $LiNi_{0.8}Co_{0.1}Mn_{0.1}O_2$ is slightly higher (203.7 mAh g^{-1}) compared to that of pristine $LiNi_{0.8}Co_{0.1}Mn_{0.1}O_2$ (198.4 mAh g^{-1}). It indicates that Ca doping does not significantly affect the initial discharge capacity. However, cycle test presents here delivers that cyclability of pristine $LiNi_{0.8}Co_{0.1}Mn_{0.1}O_2$ further worsened as the number of cycles increased. On the contrary, a relatively high cyclability of Ca-doped $LiNi_{0.8}Co_{0.1}Mn_{0.1}O_2$ is found. There is no significant difference until the 20 cycles. However, there are big difference in capacity retention after 20 cycles. The Ca-doped $LiNi_{0.8}Co_{0.1}Mn_{0.1}O_2$ demonstrates a long-term cyclability with 88.5% over 60 cycles, while pristine $LiNi_{0.8}Co_{0.1}Mn_{0.1}O_2$ provides lower capacity retention. The cyclability of PNCM is only 76.3% under the same condition. The quick capacity fading of pristine $LiNi_{0.8}Co_{0.1}Mn_{0.1}O_2$ in the cycle test is closely related to the i) increase in bond dissociation energy of Ca for Ca-doped $LiNi_{0.8}Co_{0.1}Mn_{0.1}O_2$, which is well known for long-term capacity retention of Ni-rich NCM cathode [20, 21]. The bond dissociation energy of Ca-O (ΔH_{f298} = 464 kJ mol^{-1}) is higher compared to that of Ni-O (ΔH_{f298} = 391.6 kJ mol^{-1}), Co-O (ΔH_{f298} = 368 kJ mol^{-1}) and even Mn-O (ΔH_{f298} = 402 kJ mol^{-1})

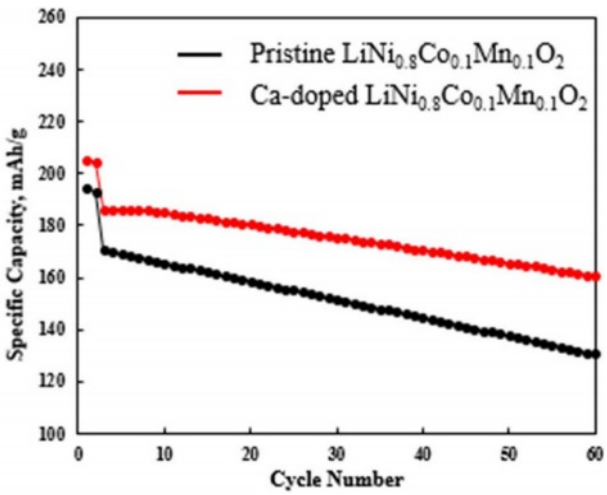

Fig. 4. Cyclabilities of pristine and Ca-doped $LiNi_{0.8}Co_{0.1}Mn_{0.1}O_2$ at 0.1 C and 0.5 C.

[22]. It leads to superior mechanical integrity, advantageous to lower internal strain and preservation of original layered structure, resulting from pillar effect of crystal structure. In addition, dopant can additionally cause the ii) enhanced electron hopping pathways and increased hopping carriers, thereby increasing the conductivity of Ca-doped $LiNi_{0.8}Co_{0.1}Mn_{0.1}O_2$ [23]. However, in case of pristine $LiNi_{0.8}Co_{0.1}Mn_{0.1}O_2$, the poor capacity retention is associated with the micro-cracking, resulting from anisotropic lattice change. The electrolyte penetration

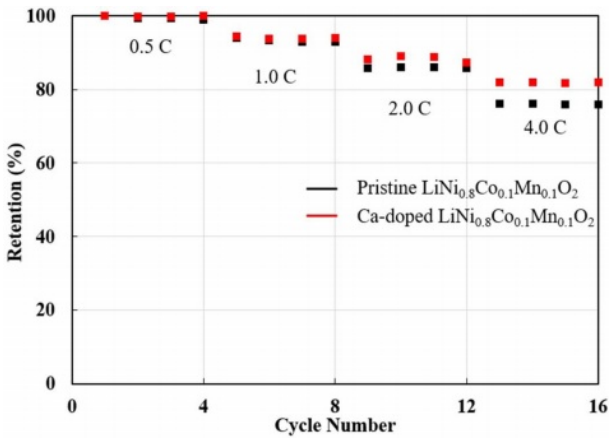

Fig. 5. Rate capabilities of pristine and Ca-doped $LiNi_{0.8}Co_{0.1}Mn_{0.1}O_2$.

to the cracks can inhibit lithium ion kinetics via unwanted solid electrolyte interface (SEI) layer on the surface of the both secondary and primary particles [15, 22]. Consequently, micro-cracking results in cycle performance degradation upon cycle test.

Moreover, the rate-performances of pristine and Ca-doped $LiNi_{0.8}Co_{0.1}Mn_{0.1}O_2$ are measured, as shown in Fig. 5 to support the advantageous of Ca doping. At low C-rate (0.5 and 1.0 C), there is no big difference between both samples. However, Ca-doped $LiNi_{0.8}Co_{0.1}Mn_{0.1}O_2$ has higher capacity retentions compared to pristine $LiNi_{0.8}Co_{0.1}Mn_{0.1}O_2$ at high C-rate (2.0 and 4.0 C). It can be elucidated by Ca doping is beneficial to good rate capability, originated from enhanced conductivity and lattice parameters.

Conclusions

The Ca-doped $LiNi_{0.8}Co_{0.1}Mn_{0.1}O_2TiO_2$ cathode material is successfully prepared via solid-state reaction to investigate the effect of Ca doping on the electrochemical performances. Although Ca-doped $LiNi_{0.8}Co_{0.1}Mn_{0.1}O_2TiO_2$ cathode material has similar morphology and average particle size, the Ca-doped $LiNi_{0.8}Co_{0.1}Mn_{0.1}O_2TiO_2$ cathode material delivers higher electrochemical performances based on better crystallization compared to pristine $LiNi_{0.8}Co_{0.1}Mn_{0.1}O_2TiO_2$ cathode material. It can be explained by wider interslab spaces and stronger bond dissociation energy of Ca-O. Therefore, we can conclude that Ca doping into the $LiNi_{0.8}Co_{0.1}Mn_{0.1}O_2TiO_2$ is one of the effective way for superior and stable electrochemical performances.

References

1. J. W. Seok, J. Lee, T. Rodgers, D. H. Ko, J. H. Shim, Trans. Electr. Electron. Mater. 20 (2019) 548-553.
2. T.T. Kojimaa, T. Ishizua, T. Horibaa, M. Yoshikawab, J. Power Sources. 189 (2009) 859-863.
3. Y. Xi, Y. Liu, D. Zhang, S. Jin, R. Zhang, M. Jin, Solid State Ion. 327 (2018) 27-31.
4. C. C. Qin, J. L. Cao, J. Chen, G. L. Dai, T. F. Wu, Y. Chen, Y. F. Tang, A. D. Li, Y. Chen, Dalton Trans. 45 (2016) 9669-9675.
5. Y. Mo, L. Guo, H. Jin, B. Du, B. Cao, Y. Chen, D. Li, Y. Chen, J. Power Sources. 448 (2020) 227439.
6. M. S. Islam, R. A. Davies, and J. D. Gale, Chem. Mater. 15 (2003) 4280.
7. F. Lin, I.M. Markus, D. Nordlund, T.C. Weng, M.D. Asta, H.L. Xin, and M.M. Doeff, Nat. Commun. 5[1] (2014) 1-9.
8. A. Manthiram, J. C. Knight, S. T. Myung, S. M. Oh, Y. K. Sun, Adv. Energy Mater. 6[1] (2016) 1501010.
9. X. Zhao, L. An, J. Sun, G. Liang, J. Electroanal. Chem. 810[1] (2018). 1-10.
10. X. Zhang, W. J. Jiang, A. Mauger, F. Gendron, C. M. Julien, J. Power Sources. 195[5] (2010) 1292-1301.
11. I. M. Makus, F. Lin, K. C. Kam, M. Asta, M. M. Doeff, J. Phys. Chem. Lett. 5[21] (2014) 3649-3655.
12. L. Yao, F. Liang, J. Jin, B. V. R. Chowdari, J. Yang, Z. Wen, Chem. Eng. J. 389 (2020) 124403.
13. W. Li, L. S. Yang, Y. X. Chen, J. Guo, J. Zhu, G. L. Cao, Ionics (Kiel). 26[11] (2020) 5393-5403.
14. S. J. Sim, S. H. Lee, B. S. Jin, H. S. Kim, Sci. Rep. 9[1] (2019) 1-8.
15. Q. Liu, Z. Zhao, F. Wu, D. Mu, L. Wang, and B. Wu, Solid State Ion. 337 (2019) 107-114.
16. S. H. Lee, B. S. Jin, H. S. Kim, Sci. Rep. 9 (2019) 17541.
17. Y. K. Li, W. X. Wang, C. Wu, and J. Yang, Trans. Electr. Electron. Mater. 23[1] (2022) 64-71.
18. S. H. Lee, H. S. Kim, B. S. Jin, J. Alloy. Comp. 803 (2019) 1032-1036.
19. S. H. Lee, S. Lee, B. S. Jin, H. S. Kim, Sci. Rep. 9 (2019) 8901.
20. S. H. Lee, G. J. Park, S. J. Sim, B. S. Jin, H. S. Kim, J. Alloy. Comp. 791 (2019) 193-199.
21. S. J. Sim, S. H. Lee, B. S. Jin, H. S. Kim, Sci. Rep. 9 (2019) 8952.
22. S. H. Lee, S. J. Sim, B. S. Jin, H. S. Kim, Mater. Lett. 270 (2020) 127615.
23. S. H. Lee, K. Y. Kim, J. R. Yoon, NPG Asia Materials 12 (2020) 28.